

Precipitation detection by the
TOPEX/Poseidon dual-frequency radar
altimeter, TOPEX microwave radiometer,
Special Sensor Microwave/Imager and
climatological shipboard reports

Damien Cailliau, Victor Zlotnicki

D. Cailliau is with the DSO/ED/AL, Département JASON-TOPEX, Centre National d'Etudes Spatiales, Toulouse, France. E-mail: dc@stormy.jpl.nasa.gov

V. Zlotnicki is with the Jet Propulsion Laboratory, California Institute of Technology, Pasadena, California. E-mail: vz@pacific.jpl.nasa.gov

Abstract

We evaluate the ability of a dual frequency (C and Ku band) radar altimeter to detect rain events. A TOPEX/Poseidon (T/P) altimeter precipitation flag for the year 1994 is compared to co-located rain rate from the Defense Meteorological Satellite Program's Special Sensor Microwave Imager (DMSP SSM/I), as processed by [1], to the TOPEX/Poseidon passive radiometer's (TMR) liquid water content, and to a 34 year climatology of shipboard present-weather reports compiled by [2]. The altimeter - SSM/I analysis is couched in terms of the tradeoff between the probability of a False Positive and the probability of a Failure to Detect rain. We show that the ability of SSM/I and TMR to detect rain are closer to each other than to either the altimeter or the shipboard climatology, especially at latitudes poleward of 45° . We argue that this is due to the inability of both radiometric techniques to detect the high latitudes snow included in the climatology, while the altimeter is sensitive to it. We also find that a TMR-only flag with liquid water content of $600 \mu\text{m}$, as used for T/P in the past several years, recovers too few rain events, $400 \mu\text{m}$ is close to climatological moderate-to-heavy intensity rains and $200 \mu\text{m}$ to rain of any intensity. We argue that a combined altimeter and TMR flag with a TMR threshold of $100 \mu\text{m}$ and the Ku radar cross section 1.5 standard deviations below an average Ku/C curve gives the most reasonable results in recovering precipitation of all types.

I. INTRODUCTION

Spaceborne altimetry is now a tool in common use for oceanographic and geophysical applications. Improving both its accuracy and the number of useful samples one satellite collects are still matters of interest. Rain influences altimetric data (e.g. [3], [4], [5]); if undetected, rain lowers the accuracy of the three quantities retrieved from altimetry: satellite range, wind speed and significant waveheight [6]. Since no current model accounts for the attenuation induced by rain droplets, such affected data are simply flagged and removed. However, this opens the possibility of using a physically distinct way to detect rain, a fundamental quantity in the hydrologic cycle and, together with evaporation, a driver of ocean motions.

TOPEX/Poseidon (T/P, launched in August 1992 and still in operation -- e.g. [8]) has two altimeters as primary instruments. In addition, it carries a passive radiometer (TMR), used primarily to correct the altimeter range for path delays due to water vapor and liquid water, and also to detect rain in the altimeter footprint. Since the NASA altimeter on T/P (called KC-ALT in the remainder) is on 90% of the time, and has two frequencies (Ku band at 13.6 GHz and C band at 5.3 GHz) to measure and correct for ionospheric

path delays, several attempts have been made to build a rain flag that takes advantage of the fact that rain attenuates the Ku signal almost 10 times more than the C signal (see [9], [10] and [11]). Except for [11] who used a climatology of shipboard rain reports from [2], these previous works could not validate such altimeter-based rain flags due to lack of other rain data.

Rain affects the quality of the retrieved altimetric range, and resulting sea level, by affecting the accuracy of two range corrections, EM-bias and path delay due to water vapor: a) rain increases the altimetrically-estimated wind speed (stronger winds lower the radar backscatter, and rain mimics this effect); a higher-than-true wind estimate yields a higher-than-true EM bias estimate; b) the algorithm used to retrieve the water vapor path is calibrated in a non scattering medium (without rain) [12], making it inaccurate in the presence of precipitation. In the case of ERS-1 and 2 the effect is more pronounced, since the on-board radiometer has only 2 frequencies, which prevents the separation of wind and water vapor in the radiometer's signal; as a consequence, the altimetric estimate of wind speed is also used to retrieve the water vapor path delay [13].

The sequence of Defense Meteorological Satellite Program's Special Sensor Microwave Imagers (DMSP SSM/I) has collected, since 1987, a remarkable long time series of observations. As processed by [1], the retrievals include wind speed at the ocean surface, and water vapor, rain rate and liquid water in the atmospheric column above, all retrieved consistently across the various spacecraft. We thus chose to compare the KC-ALT rain flag against co-located SSM/I.

As shown below, however, we found systematic differences at high latitudes between the 'rain' detection abilities of SSM/I (with current algorithms) on the one hand, and KC-ALT on the other, differences similar to those found by [2] and [14] in comparing other SSM/I retrievals with his carefully-constructed climatology of shipboard present-weather rain reports. By using also the TMR rain flag, we show that the systematic differences are common to both passive radiometers, whereas KC-ALT's precipitation detection better matches the high latitude behaviour of an in-situ precipitation climatology when the phase 'snow' is included in the climatology.

The Tropical Rainfall Measuring Mission (TRMM), launched in October 1997, will likely

bring tremendous improvements in rain detection [15]. To date, however, few results are available, and only in the tropical regions ($+/- 35^\circ$), so we could not use it in our comparisons.

II. DATA

A. The Altimeter Rain Flag

The TOPEX/Poseidon data we use are the Merged Geophysical Data Records version 'B' (MGDR-B), released in 1997, described in [16] and available from <http://podaac.jpl.nasa.gov>. However, we use only cycles where the NASA dual-frequency altimeter (KC-ALT) was in operation (about 90% of the time).

The key rain flag we evaluate uses a combination of KC-ALT and TMR. The radar altimeter's backscatter coefficient σ_0 measures the power returned from the ocean surface relative to that sent out by the altimeter (e.g., [7]) at a particular frequency, and it primarily measures wind speed, whose roughening of the ocean surface scatters away energy at radar frequencies. Following [10], we constructed a mean curve of σ_0^K (13.6 GHz) vs σ_0^C (5.3 GHz). Such a relationship attempts to represent the ratio between the backscatter coefficients free of both noise and rain, according to the editing. We used cycles of KC-ALT, for the months of January, April, July and October of the years 1993, 1994, and 1995, whose data survived the editing criteria described in [16] and [9]:

- TOPEX is ON,
- Attitude is $< 0.1^\circ$,
- Minimum of 6 valid 10Hz measurements in the sample,
- All bits of Alt_Bad_1 and Alt_Bad_2 are set to 0,
- TMR is neither over land nor over ice, with good quality,
- $LWP < 200\mu\text{m}$,
- Use of the backscatter coefficients *not* corrected for atmospheric attenuation.

Although constructed from different times, with somewhat different editing criteria, our relationship (Fig 1) shows few differences from those obtained by [9] or [10].

A rain detection event is defined to occur when:

$$\begin{cases} f(\sigma_0^C) - \sigma_0^K > th \cdot rms(\sigma_0^C) \\ LWP > LWP_{th} \end{cases} \quad (1)$$

With σ_0^C and σ_0^K the observed backscatter coefficients, $f()$ the C/Ku relationship in Fig 1, $rms()$ the standard deviation of the relationship, LWP the Liquid Water Path as measured by TMR; the two thresholds to be 'tuned' are th and LWP_{th} .

Please note that each σ_0 sample is an average over an area whose diameter is about 2 to 12 km, larger when the waveheight in the footprint is larger [17].

B. TMR Rain Flag

The Topex microwave radiometer (TMR, see [18] and [19]) is on the same T/P satellite as the KC-ALT described above and its data are on the same MGDR-B dataset. TMR measures the sea surface brightness temperature at 18, 21, and 37 GHz, all horizontally polarized. TMR's representative footprint is roughly 40 km [20]. The algorithms used to process the path delays are described in [12].

The TMR rain flag in the MGDR-B is set if [21] :

- (i) Any one brightness temperature is out of range ([100 K, 208 K] for Tb18, [105 K, 238 K] for Tb21, [130 K, 258 K] for Tb37).
- (ii)

$$LWP \geq R_{th} \quad (2)$$

Where LWP is the Liquid Water Path in micrometers, and R_{th} is a threshold. The assumption is that high LWPs are caused by rain in the beam.

In the MGDR-A dataset (released in 1993) the threshold was 1000 μm ; in MGDR-B (released in 1997) a threshold of 600 μm is used [16]. This 'rain flag' is what almost all users of T/P data use.

C. DMSP SSM/I

The SSM/I senses the brightness temperature at frequencies of 19V, 19H, 22V, 37V, 37H, 85V GHz (V and H refer to vertical and horizontal polarization). We used the files of SSM/I parameters, sampled daily, on a $0.25^\circ \times 0.25^\circ$ grid, which include rain rate, from DMSP satellites F10 and F11, computed by [1] and available from <http://www.ssmi.com>.

Since using KC-ALT we are only defining a yes/no rain occurrence, we took any SSM/I rain rate higher than 0.2mm/hr as a rain event, (F. Wentz, personal communication, [1998]; the data are quantized at 0.1 mm/hr). Although there is a sample every 0.25° , each is a weighted average over an area approximately 30 to 60km in diameter, depending on the channel.

D. Shipboard Rain Climatology

We used the climatology of shipboard present-weather rain reports compiled by [2] and available from <http://ncar.ucar.edu/dss/datasets/ds541.2.html>. It consists of ship precipitation frequencies, in boxes $2.5^\circ \times 2.5^\circ$ over the 34 year span 1958–1991. Our study lead us to differentiate the climatology corresponding to all precipitation classes (i.e. phase classes: indeterminate or hail, liquid, snow and trasition; the latter includes mixed phase or freezing precipitation or sleet) from the one excluding snow (all previous phase classes except snow). Furthermore, as did [2], we organized our results in 3 categories distinguished by the intensity of precipitation: all local precipitation (groups 7, 10–12, 14–31 for all precipitation phases; groups 7, 10, 12, 14–18, 21–27, 30–31 w/out snow), precipitation greater than drizzle intensity (groups 7, 14–31 for all precipitations phases; groups 7, 14–18, 21–27, 30–31 w/out snow), and precipitation of moderate to heavy intensity (groups 23–31 for all precipitations phases; groups 23–27, 30–31 w/out snow). The reader is referred to [2] and [14] for important details and warnings concerning these data.

E. Ice Edge

Because the main discrepancy between the altimetric and passive radiometer flags are found at higher latitudes, it is essential to edit out suspected ice samples carefully. In addition to the ice flags in both the SSM/I and T/P data, we edited out of any comparison, samples poleward of a 6 day average 15% ice contour of the Antarctic, processed by the National Snow and Ice Data Center's data (NSIDC) generally based on SSM/I data.

III. TOPEX/POSEIDON CROSSOVERS WITH DMSP SSM/I

A. Method

For the comparison, we used only data covering the year 1994 [T/P cycles 48–84, except 55, 65, 79] and the corresponding SSM/I daily maps. A co-located pair T/P and SSM/I was defined to occur when the nominal latitude-longitude of the T/P KC-ALT's sample was inside the $0.25^\circ \times 0.25^\circ$ SSM/I sample, and when their times differed by no more than 30 minutes.

A classical statistical way to compare a yes/no detection criterion to another one considered as 'truth', requires computation of two competing quantities: the probability of a False Positive and the probability of a Failure to Detect [22] —hereafter FP and FTD—, often used in medical test evaluation. This approach highlights the inherent tradeoff in any flagging scheme between increased sensitivity (which minimizes the failure to detect) and the price paid by raising the number of false alarms, which in the case of altimetry results in unnecessarily removed samples.

We applied this method to the KC-ALT flag, as if the SSM/I data were 'truth'. The probability of a False Positive is estimated as the ratio between the number of matching TOPEX points that indicate the presence of rain [with a particular set of rain flag parameters] while the corresponding SSM/I pixel shows no rain or some ice, divided by the total number of TOPEX point indicating the presence of rain. The probability of a Failure to Detect is estimated as the ratio between the number of matching SSM/I pixels indicating the presence of rain while *none* of the corresponding TOPEX samples' rain flag is set, divided by the total number of SSM/I matching pixels indicating the presence of rain.

B. Results and discussion

Fig 2 shows in the (FP, FTD) space the results for both TMR (in blue) and KC-ALT + TMR (other colors) rain flags, as a function of their leading parameter (R_{th} for TMR, th for the KC-ALT, see (2) and (1)), and for several latitudinal bands. The thick solid curves represent the global performances, while the thin solid, dashed, dot-dashed, etc. lines represent the performance for specific latitude bands [see Fig 2's caption for details]. The large continental mass over 50° N precludes a reliable curve for this latitude band.

Finally, two global curves are presented for the KC-ALT flag, each one corresponding to a different value of the secondary parameter, LWP_{th} [$0\mu\text{m}$; $200\mu\text{m}$].

Fig 2 shows that, if SSM/I were the truth, TMR would always give better performance than KC-ALT's flag; notice that whether FP or FTD are considered, the TMR curves are always closer to SSM/I (the origin point of the plot). Furthermore, although TMR performance (relative to a 'true' SSM/I) does not change much with latitude, the KC-ALT flag departs further from the SSM/I 'truth' when going poleward. Finally, it is impossible to define for the KC-ALT flag a set of parameters that give both low FP and low FTD relative to SSM/I, while TMR shows a best match to the SSM/I 'truth' for a threshold of $400\mu\text{m}$. Several possibilities may explain these discrepancies.

Consider first the difference in resolution between SSM/I, TMR and KC-ALT. While the first two are comparable (30 to 60 km and 40 km, respectively), the latter has far higher resolution (from 2 km to 12 km footprint, depending on the wave height). Due to the averaging over the footprint, it is quite possible that KC-ALT—if perfect—would detect a small rain cell raining at, say, the light-rain rate of 3 mm/hr, but when averaged over the larger passive radiometer footprint would appear as 0.1 mm/hr, at the edge of SSM/I or TMR sensitivity. On the other hand, it is also possible that SSM/I and TMR detect some rain inside their footprint but outside the KC-ALT footprint. We could not quantify these uncertainties, as that would require a reliable estimate of the probability density of rain cells vs their horizontal extent and rain rate, preferably as a function of latitude.

Consider next the possibility put forth by [14]: he found that rain frequencies from many of the 10 rain detection algorithms for SSM/I he considered (the Wentz product [1] used here is not among them) for August–November, 1987, showed decreasing rain frequency at high latitudes, even for moderate to heavy intensity, just the opposite of the shipboard climatology. He argued that the lower column of water vapor and the presence of frozen precipitation (snow) associated with colder high latitudes, would confuse algorithms tuned to retrieve light precipitation in the lower, more humid latitudes, especially if they did not account for water vapor. However, Wentz's algorithm does, since vapor, wind, rain rate and liquid water are simultaneously estimated.

As we will see in the next section, another source of differences is the type of precipitation: at the higher latitudes snow, rather than liquid rain is the prevalent mode of precipitation.

Because we find that the performance of the KC-ALT flag relative to SSM/I rain rate $> 0.2\text{mm.h}^{-1}$ changes with latitudes, while the TMR flag does not (Fig 2), in the next section we consider another data type in order to assess the reason.

IV. COMPARISON WITH CLIMATOLOGICAL STUDIES

We now focus on the high latitude differences. Since SSM/I is not perfect and no other global, contemporaneous, frequently sampling, rain data set is available, we tested the KC-ALT results against a compilation of climatological shipboard reports [2]. Notice that such a comparison must focus on broad statistical properties of each dataset, as it is not possible to co-locate the data in space and time to analyze their differences. What we now consider 'truth' are these broad statistical properties of the ship climatology.

The widely used climatologies of local precipitation rate are based on rain gauges, satellite observations of passive radiometer or infrared type, or a combination thereof (e.g. [23], [24], [25], [26]). Our rain flags are not calibrated to recover precipitation rates, only whether-or-not rain is present, thus we used a climatology of precipitation frequency. The shipboard reports compiled by [2] provide excellent oceanic coverage and allow us to discuss precipitation frequency (see [2] and [14] for important warnings on the accuracy of this climatology).

There is an important distinction between precipitation rate and frequency. Generally speaking, the zonally-averaged profile of annual rain rate versus latitude from [26] shows a characteristic three peak structure: the near-equatorial peak is the largest, with 5.5 mm/day, centered around 5°N; the secondary peaks are 3.5 mm/day at 40-50°S and 2.5 mm/day at 40-50°N; precipitation at 70°N or S is at most 1 mm/day. Although values and latitudes differ some, [24] has the same structure. Rain frequency from ship reports [2], shown in the thick blue lines of Fig. 3 also has the characteristic three peak structure, with the peaks at about the same latitude bands, but the high latitude peaks are larger than the near-equatorial peak: rain is more frequent but less intense at high latitudes. The distinction between the three blue curves in all panels of Fig. 3 is intensity. The lowest

curve includes only ship reports of local precipitation of moderate to heavy intensity, the intermediate curve has at least “drizzle” intensity, and the upper curve is local precipitation of any intensity. Their common theme is that they do not include ‘snow’. By contrast, the blue curves in Fig. 4 correspond to the same intensity definitions, but include the class ‘snow’, and the mid-latitude peaks disappear, as precipitation frequency continues to increase with latitude.

We then generated latitudinal rain frequencies from the KC-ALT+TMR flag, from the TMR-only flag, and from the SSM/I rain rate flag in 2.5° latitudinal bins, for various values of their unknown threshold parameters. We compared these curves with the ship report frequencies from [2], as shown in Fig. 4 for all precipitation including snow, and with ship reports for all precipitation excluding snow, Fig. 3.

The KC-ALT-only flag (setting TMR’s $LWP_{th} = 0 \mu\text{m}$, Fig 4.a), recovers very well the increase with latitude (poleward of about 30°) in frequency of all precipitation including snow, but overestimates rain frequency in the tropics. Conversely, the TMR-only flag (Fig 4.d) fails to account for this steady increase poleward of 50°S and 45°N , but matches very well the curves of precipitation excluding snow (Fig 3.d). The same remarks apply to the SSM/I results (green curve in Fig 4.d and 3.d), even though one can notice a slight over estimation around the ITCZ. This leads us to conclude that the KC-ALT is affected by what is classified as snow at the sea surface, while the radiometer techniques are only sensitive to liquid precipitation.

Although dry snow attenuates the Ku-band radar signal an order of magnitude less than rain does, at the same precipitation rate ([27], [28]), heavy snowfall does have a significant influence on Ku-band. Furthermore, [27] reports that some wetness in the snowflakes greatly increases their attenuation of radar waves, making wet snow a medium with greater attenuation than rain, at the same precipitation rate.

Does snow appear in the more traditional climatologies of precipitation rate, such as [24] or [26] ? To the extent they include radiometer data, they would likely have the same bias shown here for TMR or SSM/I. An important data source in those climatologies are rain gauges, which can have 80% error in measuring snow rate according to [24]. We thus limit our comparisons to Petty’s climatology [2] of all precipitation phases, i.e. including

snow.

For the KC-ALT flag alone (with $LWP_{th} = 0\mu\text{m}$, Fig 4.a) the best match occurs with $th = 2.0$, close to climatological “moderate/heavy intensity” precipitation, with a lower under-estimation at high latitude than other thresholds.

The combined KC-ALT + TMR flag (non-zero LWP_{th} , Fig. 4.b and 4.c) flattens the high latitude tails and lowers the fraction of precipitation recovered. The combination $LWP_{th} = 100\mu\text{m}$ and $th = 1.5$ best matches the heavy/moderate climatological precipitation curve, while slightly over-estimating tropical rain. Using $LWP_{th} = 200\mu\text{m}$ severely flattens the curves at high latitudes (poleward of 45N and 50S) and makes the flag useless to detect lighter precipitations (we consider any value of $th < 1$ an unreasonable threshold, for obvious statistical reasons).

The TMR-only flag with $R_{th} = 200\mu\text{m}$ (Fig. 4.d) gives a surprisingly good match in [50S;45N] to overall local precipitation and an even better match to precipitation excluding snow; it slightly under-estimates near 10S. The TMR-only curve for $R_{th} = 400\mu\text{m}$ matches, albeit less well, the climatological moderate-heavy precipitation frequency, over a narrower latitude range. In the previous section we showed that $R_{th} = 400\mu\text{m}$ was the best match to co-located SSM/I rain detection. The $600\mu\text{m}$ threshold used currently in the T/P MGDR-B severely under-estimates precipitation at all latitudes.

V. DISCUSSION AND CONCLUSIONS

By comparing Fig 4.a and 3.a, one may conclude that what is classified as snow in the ship reports climatology affects the altimeters (attenuates the Ku-band signal). In the context of the quality of retrieved range in an altimeter dataset, this is a useful fact and cannot be ignored.

Also from Fig. 4.a-d, one can draw several conclusions. First, while combining TMR with KC-ALT lowers the number of precipitation events detected relative to what KC-ALT alone detects, it is not obvious that the events thus removed are false positives. On purely statistical considerations one would choose a value of $th \gg 1$, calling “precipitation” only cases where σ_0^K is much more than one standard deviation below the curve for normal, dry conditions. The KC-ALT-only curve with $th = 2$, $LWP_{th} = 0$ in Fig. 4.a is not significantly different in shape from the climatological curve for moderate-to-heavy intensity;

while lower values of th lead to a clear overestimation at low latitudes relative to other locations, one can argue that the stricter probabilistic threshold $th = 2$ does an excellent job of removing false positives without additional information from TMR. Furthermore, as Fig. 4.c clearly shows, $LWP_{th} = 200\mu\text{m}$ is an upper bound on the TMR restriction for a KC-ALT + TMR flag; higher values of LWP_{th} would simply make a combined flag too insensitive to even moderate to heavy rains.

There are simple reasons for KC-ALT to detect precipitation events that TMR or SSM/I do not. When the horizontal extent of a contiguous rain patch is small, let us say 6 km in 'diameter', a respectable rain rate of $\approx 4.9\text{mm/hr}$ appears, when averaged over an otherwise dry 40 km footprint, as $\approx 0.1\text{mm/hr}$; the same logic gives a low amount of liquid water when averaged over the TMR footprint.

Furthermore, consider this: both TMR alone with $R_{th} = 200\mu\text{m}$ and KC-ALT alone with $th = 1.0$ recover about the same precipitation frequencies as a function of latitude that climatology labels 'all precipitation'. However, the combined flag with $th = 1.0$ and $LWP_{th} = 200\mu\text{m}$ recovers about five times fewer events (Fig. 4.a,d,c), and the events TMR recovers are "closer" to those SSM/I recovers than to those KC-ALT does (Fig 2). One possible explanation for this pattern is that the Altimeter flags events too small to be detected by TMR, and TMR (or SSM/I) detects events in its footprint but outside the Altimeter footprint. This also justifies using a low value of LWP_{th} in any assumed KC-ALT + TMR flag.

Finally, as discussed in Section IV, at high latitudes KC-ALT appears to detect snow events to which the radiometer techniques are blind. Thus, a combined TMR and KC-ALT flag would tend to miss snow events, as the TMR contribution is increased. If recovering snow is of interest, it is necessary to keep LWP_{th} very low.

The False Positive / Failure to Detect approach we used to compare KC-ALT with SSM/I, summarized in Fig 2, better illustrates the tradeoff incurred by moving threshold values than other approaches, but cannot be interpreted as such because SSM/I is not really the "truth" of what KC-ALT measures. The main conclusion from Fig 2 is that there exist systematic similarities in the what TMR and SSM/I measure and systematic differences between either of them and KC-ALT.

This work also showed that the current TMR-only rain flag used in the TOPEX/Poseidon MGDR, set when TMR's Liquid Water Path exceeds $600 \mu\text{m}$, misses most of even the heaviest rains (Fig. 4.d and 3.d) (it flags roughly 2% of the TOPEX samples, Fig 5). Presumably this underestimation of rain events was worse with the $1000 \mu\text{m}$ threshold used in MGDR-A (the T/P dataset made available in 1993, just after the calibration phase). Although we also showed that a TMR-only flag with $R_{th} = 200 \mu\text{m}$ matches extremely well climatological rain of any intensity, at least equatorward of 50° latitude, we would not recommend such a threshold for a TMR-only rain flag for altimetry, since it would remove 16% of T/P KC-ALT samples, and in most cases the rain would be in the TMR footprint but not necessarily in the KC-ALT footprint. So, if a TMR-only rain flag for altimetry is needed, as is the case for the CNES altimeter aboard T/P, as well as for ERS-2 and other single-frequency altimeters, then it appears that $R_{th} = 400 \mu\text{m}$, which flags about 5% of the T/P KC-ALT samples, provides a more appropriate tradeoff. Notice that this threshold looks appropriate in both the comparison to shipboard climatology and in the co-located comparison to SSM/I. The fact remain, however, that high latitudes snowfall that could affect the altimeter will be missed in a radiometer-only flag.

When a combined KC-ALT + TMR flag can be computed and is desired, we would recommend $th = 1.5$ and $LWP_{th} = 100 \mu\text{m}$, which best recovers the climatological moderate to heavy intensity precipitations of all phases (Fig 4.a), and removes approximately 6% of T/P samples.

Both the TMR liquid water product and the SSM/I rain-rate product used here fail to correctly reproduce the increase in all-precipitation frequency with latitude at high latitudes, a fact noted by [2] and [14] for many SSM/I products. However, the explanation given by [14] for this failure, that water vapor was not solved for in the algorithms, does not seem to apply here since the TMR retrieval is of both liquid water and water vapor, and Wentz's SSM/I product solves simultaneously for rain rate, water vapor, liquid water and wind. As we argued above, a clue to explain this behaviour may lie in the radiometer's inability to sense snow.

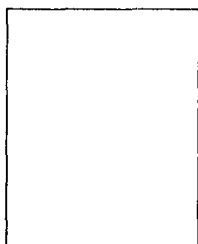
ACKNOWLEDGMENTS

We are grateful to Merick Srokosz and Ziad Haddad for very helpful remarks, Xiang Liu for the Antarctic 6 day ice contours, Remote Sensing Systems for the SSM/I products, and NCAR for [2]'s climatology. We are also grateful to CNES and especially Dr. Yves Menard for supporting D. Cailliau's stay at JPL, and to NASA/EOSDIS/PO-DAAC for supporting V. Zlotnicki. This work was performed at the Jet Propulsion Laboratory, California Institute of Technology, under contract with the National Aeronautics and Space Administration.

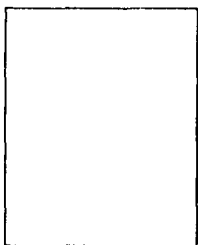
REFERENCES

- [1] Wentz, F. J., R. W. Spencer, SSM/I rain retrievals within a unified all-weather ocean algorithm, *RSS Tech. Rep. 120196*, 31 pp, Remote Sensing Systems, Santa Rosa, Calif., 1996.
- [2] Petty, G. W., Frequencies and characteristics of global oceanic precipitation from shipboard present-weather reports, *Bull. Am. Meteorol. Soc.*, Vol. 76, No. 9, 1593-1616, 1995.
- [3] Goldhirsh, J., J. R. Rowland, A tutorial assessment of atmospheric height uncertainties for high-precision satellite altimeter missions to monitor ocean currents, *IEEE Trans. on Geos. and Rem. Sens.*, Vol GE-20, No. 4, 418-433, 1982.
- [4] Walsh, E. J., F. M. Monaldo, J. Goldhirsh, Rain and cloud effects on a satellite dual-frequency radar altimeter system operating at 13.5 and 35 GHz, *IEEE Trans. on Geos. and Rem. Sens.*, Vol GE-22, No. 6, 615-622, 1984.
- [5] Guymer, T. H., G. D. Qualtry, M. E. Srokosz, The effects of rain on ERS-1 radar altimeter data, *J. Atm. Ocean. Tech.*, 12, 1229-1247, 1995.
- [6] Chelton, D. B., WOCE/NASA altimeter algorithm workshop, *U.S. WOCE Tech. Rep. 2*, 70 pp, Oregon State University, Corvallis, Oreg., 1987.
- [7] Chelton, D. B., E. J. Walsh, J. L. MacArthur, Pulse compression and sea level tracking in satellite altimetry, *J. Atm. Ocean. Tech.*, 6, 407-438, 1989.
- [8] Fu, L.-L., E.J.Christensen, C.Yamarone, M.Lefebvre, Y.Menard, M.Dorrer and P.Escudier: TOPEX/POSEIDON Mission Overview *J.Geophys.Res.*, 99 (C12) 24369-24381, 1994.
- [9] Qualtry, G. D., T. H. Guymer, M. A. Srokosz, The effects of rain on Topex radar altimeter data, *J. Atm. Ocean. Tech.*, 13, 1209-1229, 1996.
- [10] Tournadre, J., J. C. Morland, The effects of rain on TOPEX/Poseidon altimeter data, *IEEE Trans. on Geosc. and Rem. Sens.*, Vol. 35, No. 5, 1117-1134, 1997.
- [11] Chen, G., B. Chapron, J. Tournadre, K. Katsaros, D. Vandemark, Global oceanic precipitation: a joint view by TOPEX and the TOPEX microwave radiometer, *J. Geophys. Res.*, Vol. 102, No. C5, 10457-10471, 1997.
- [12] Keihm, S. J., M. A. Janssen, C. S. Ruf, TOPEX/Poseidon Microwave radiometer (TMR): III. Wet troposphere range correction algorithm and pre-launch error budget, *IEEE Trans. on Geos. and Rem. Sens.*, Vol. 33, No. 1, 147-161, 1995.
- [13] Eymard, L., L. Tabary, A. Le Cornec, The microwave radiometer on board ERS-1: Part 2-validation of the geophysical products, *IEEE Trans. on Geos. and Rem. Sens.*, Vol. 32, No. 2, 291-303, 1996.

- [14] Petty, G. W., An intercomparison of oceanic precipitation frequencies from 10 special sensor microwave/imager rain rate algorithms and shipboard present weather reports, *J. Geophys. Res.*, Vol. 102, No. D2, 1757-1777, 1997.
- [15] Theon, J. S., The Tropical Rainfall Measuring Mission (TRMM), *Adv. in Space Res.*, Vol. 14, No. 3, 159-165, 1993.
- [16] Benada, J. R., Merged GDR (TOPEX/Poseidon) generation B User's handbook, *Physical Oceanography Distributed Active Archive Center Po.DAAC, Ver. 2.0*, Jet Propulsion Lab., Pasadena, Calif., 1997.
- [17] Marth, P. C., J. R. Jensen, C. C. Kilgus, J. A. Perschy, J. L. MacArthur, D. W. Hancock, G. S. Hayne, C. L. Purdy, L. C. Rossi, C. J. Koblindky, Prelaunch performance of the NASA altimeter for the TOPEX/Poseidon project, *IEEE Trans. on Geos. and Rem. Sens.*, Vol. 31, No. 2, 315-332, 1993.
- [18] Ruf, C. S., S. J. Keihm, M. A. Janssen, TOPEX/Poseidon Microwave radiometer (TMR): I. Instrument description and antenna temperature calibration, *IEEE Trans. on Geos. and Rem. Sens.*, Vol. 33, No. 1, 125-137, 1995.
- [19] Ruf, C. S., S. J. Keihm, B. Subramanya and M. A. Janssen, TOPEX/Poseidon Microwave radiometer performance and in-flight calibration, *J. Geophys. Res.* 99 (c12), 24,915-24,926, 1994.
- [20] Janssen, M. A., C. S. Ruf, S. J. Keihm, TOPEX/Poseidon Microwave radiometer (TMR): II. Antenna pattern correction and brightness temperature algorithm, *IEEE Trans. on Geos. and Rem. Sens.*, Vol. 33, No. 1, 138-146, 1995.
- [21] Callahan, P. S., S. N. Rosell, D. R. Royer, L-L. Fu, A. R. Zieger, TOPEX ground segment science algorithm specification, *TOPEX/Poseidon Project JPL D-7075, Rev. A, Change 1*, Jet Propulsion Lab., Pasadena, Calif., 1990.
- [22] Larsen, R. J., M. L. Marx, *An introduction to mathematical statistics and its applications*, 536 pp., Prentice-Hall, Inc., Englewood Cliffs, N.J., 1981.
- [23] Spencer, R. W., Global oceanic precipitation from the MSU during 1979-92 and comparisons to other climatologies, *J. of Climate*, Vol. 6, 1301-1326, 1993.
- [24] Legates, D. R., C. J. Wilmott, Mean seasonal and spatial variability in gauge-corrected, global precipitation, *Int. J. of Climato.*, Vol. 10,, 111-127, 1990.
- [25] Huffman, G. J., R. F. Adler, P. Arkin, A. Chang, R. Ferraro, A. Gruber, J. Janowiak, A. McNab, B. Rudolf, and U. Schneider, The Global Precipitation Climatology Project (GPCP) combined dataset, *Bull. Amer. Meteorol. Soc.*, Vol. 78, No. 1, 5-20, 1997.
- [26] Jager, L., Monthly and areal patterns of mean global precipitation in *Variation in the Global Water Budget*, A. Street-Perrott, D. Reidel, 129, 1983.
- [27] Oguchi, T., Electromagnetic wave propagation and scattering in rain and other hydrometeors, *Proceedings IEEE*, Vol. 71, No. 9, 1029-1078, 1983.
- [28] Ulaby, F. T., R. K. Moore, A. K. Fung, *Microwave Remote Sensing - Active and passive*, Vol. 1, 456 pp., Addison-Wesley Publishing Co., Reading, Mass, 1981.



Damien Cailliau received the engineer diploma from Institut Supérieur d'Electronique du Nord, Lille, France, in electronics, in 1996. He received the Diplôme d'Etudes Approfondies from the Université de Paris 6, Paris, France, in Astronomie and Space instrumentation, also in 1996. In 1997, he joined the Département JASON-TOPEX of the Centre National d'Etudes Spatiales, France. He was a visiting scientist at the Jet Propulsion Laboratory for the time of this study.



Victor Zlotnicki (M'86) studied Surveying and Geophysical Engineering at University of Buenos Aires, Argentina, and received the Ph.D. in Oceanography from Massachusetts Institute of Technology and Woods Hole Oceanographic Institution in 1983. He has been with the Jet Propulsion Laboratory, California Institute of Technology since 1985. His present research interests include applications of altimetry and gravimetry to ocean circulation, accuracy improvements for altimetric data, and the processing and management of large satellite datasets.

Fig. 1. Relationship between Radar Cross Section (σ) at C and Ku bands. Processed over 12 cycles, one per season of the years 1993, 1994, 1995. The solid line is the average relationship, dotted is ± 1 standard deviation; the standard dev. itself is the thick gray line, whose axis is on the right.

Fig. 2. False-Positive (FP) vs Failure-to-Detect (FTD) probabilities for KC-ALT and TMR flags, assuming SSM/I is "truth". TMR-only curves in blue, for 4 latitude bands and global, parameterized with R_{th} . KC-ALT + TMR ($LWP_{th} = 200\mu m$) curves in red, for the same latitude bands, parameterized by th . KC-ALT only, global, in green. The latitude bands are: tropical [30S;30N], mid-south [50S;30S], mid north [30N;50N], and polar south [66S;50S].

Fig. 3. Zonally-averaged precipitation frequencies. KC-ALT flag only (red lines in (a)), KC-ALT + TMR (red lines in (b), (c)), TMR-only (red lines in (d)) and SSM/I (green line in (d)). Ship climatology (blue lines in (a)-(d)). The climatological curves correspond to all precipitation phases, EXCLUDING snow. The three curves correspond to different intensity levels: upper - all precipitation, middle - precipitation greater than "drizzle" intensity, lower- precipitation of moderate to heavy intensity. The KC-ALT curves are labelled with the value of th (equation 1), the TMR-only curves with the value of R_{th} (equation 2). The KC-ALT, TMR and SSM/I flags are for 1994. All frequencies averaged over 2.5° latitudinal bins.

Fig. 4. Idem as Fig 3, except the climatology curves (blue thick lines) include snow.

Fig. 5. Global fraction of TOPEX points removed by the KC-ALT flag only, KC-ALT + TMR flag (black lines), and TMR-only flag (gray line, upper axis), processed for 1994. The KC-ALT only and KC-ALT + TMR curves are parametrized by LWP_{th} .

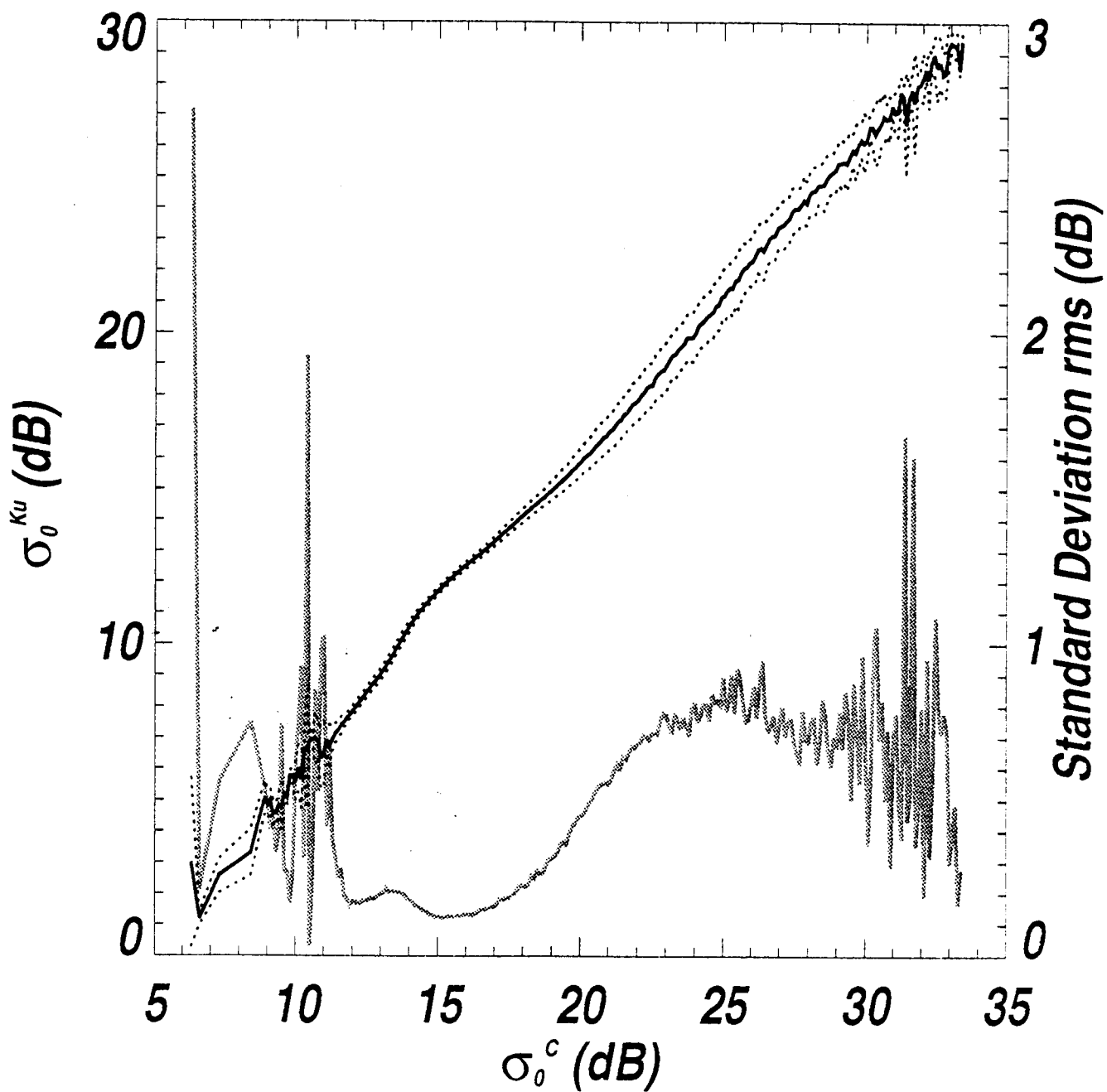


Fig 1

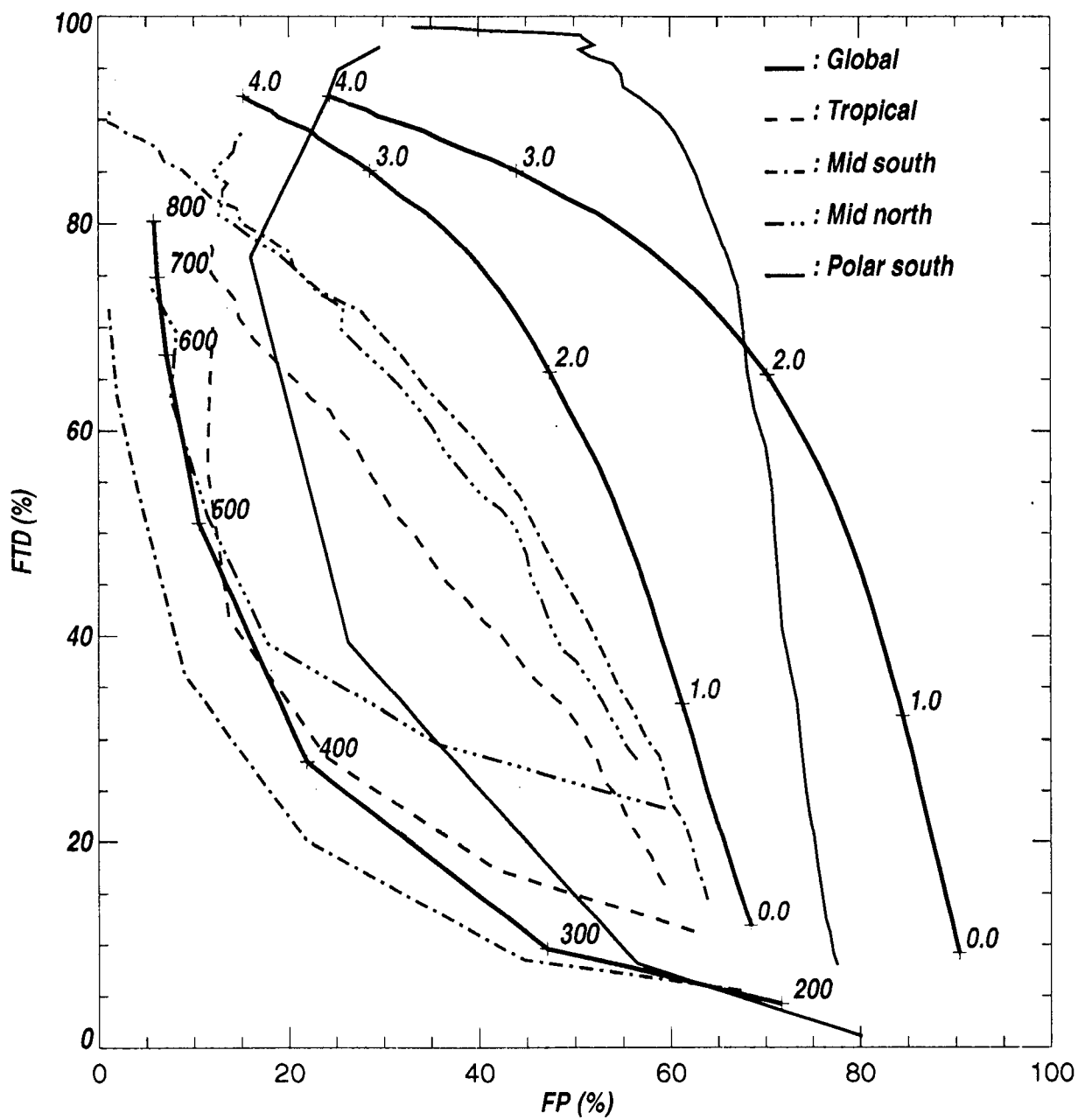


Fig 2
 dec 1981-1982

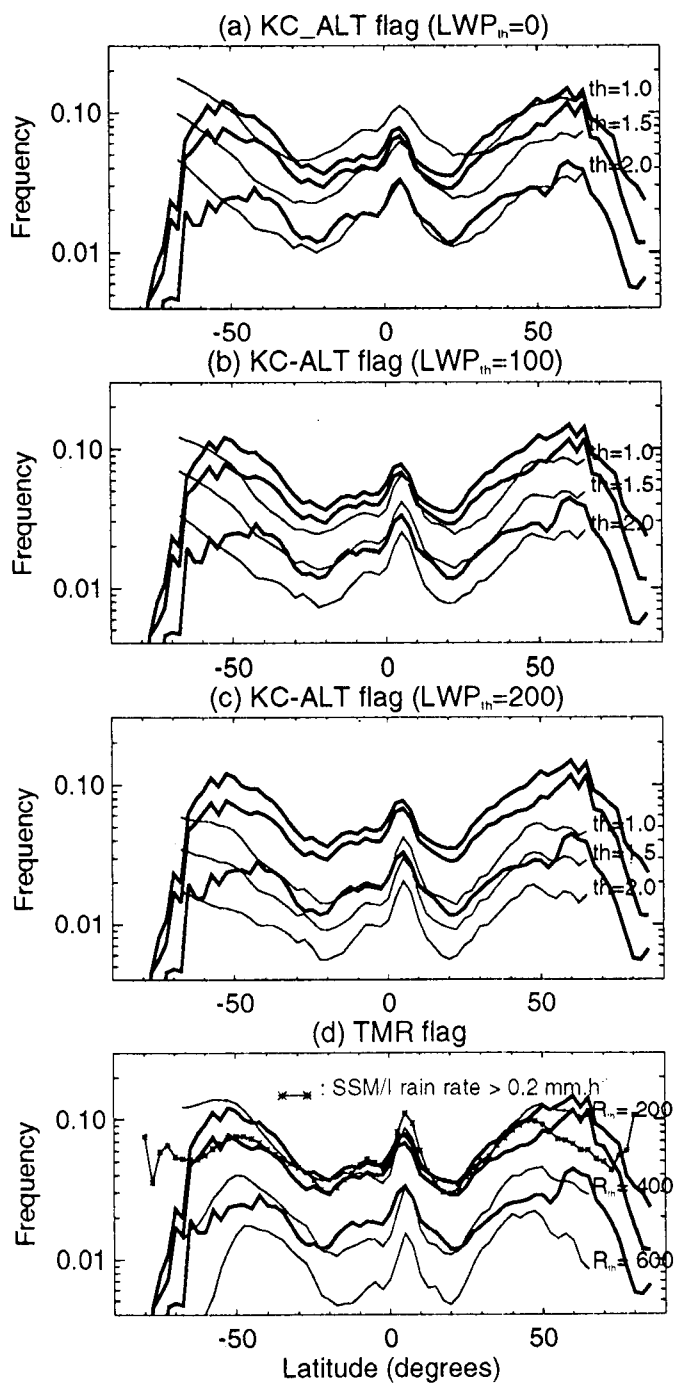


Fig 3

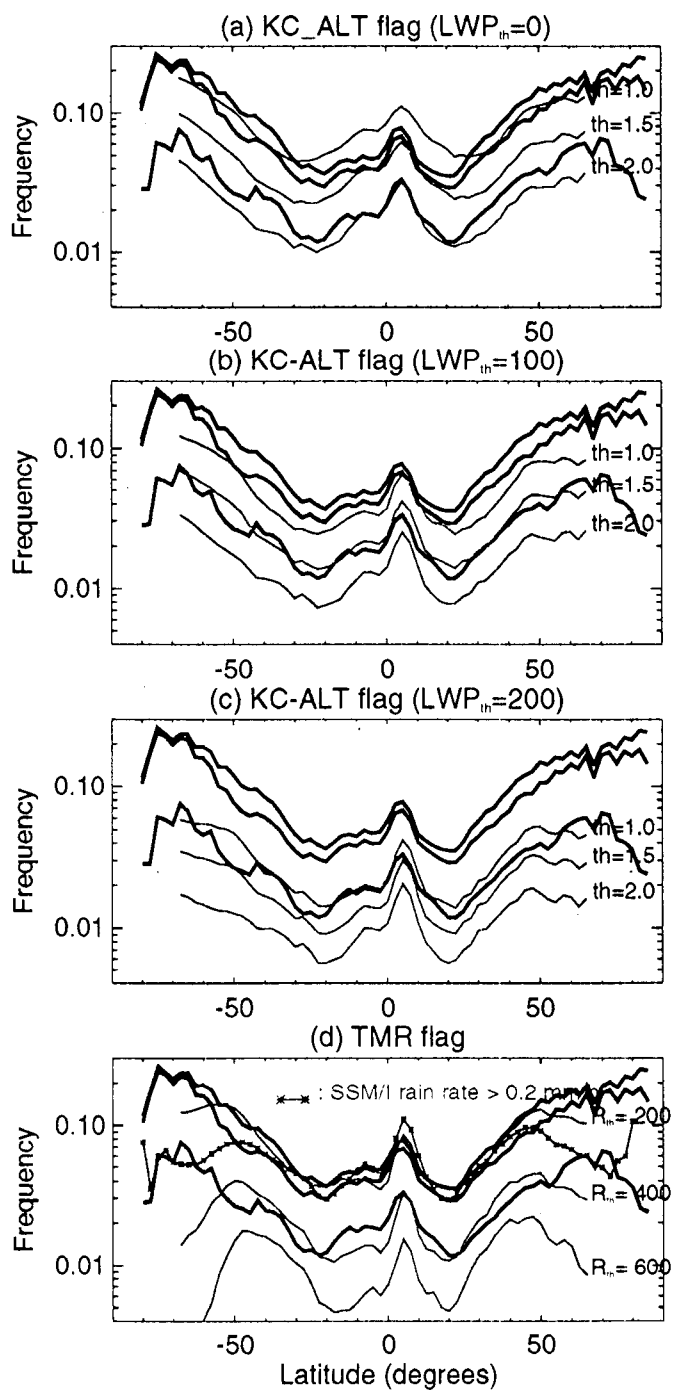


Fig 4

dc & vz - 8/06/98

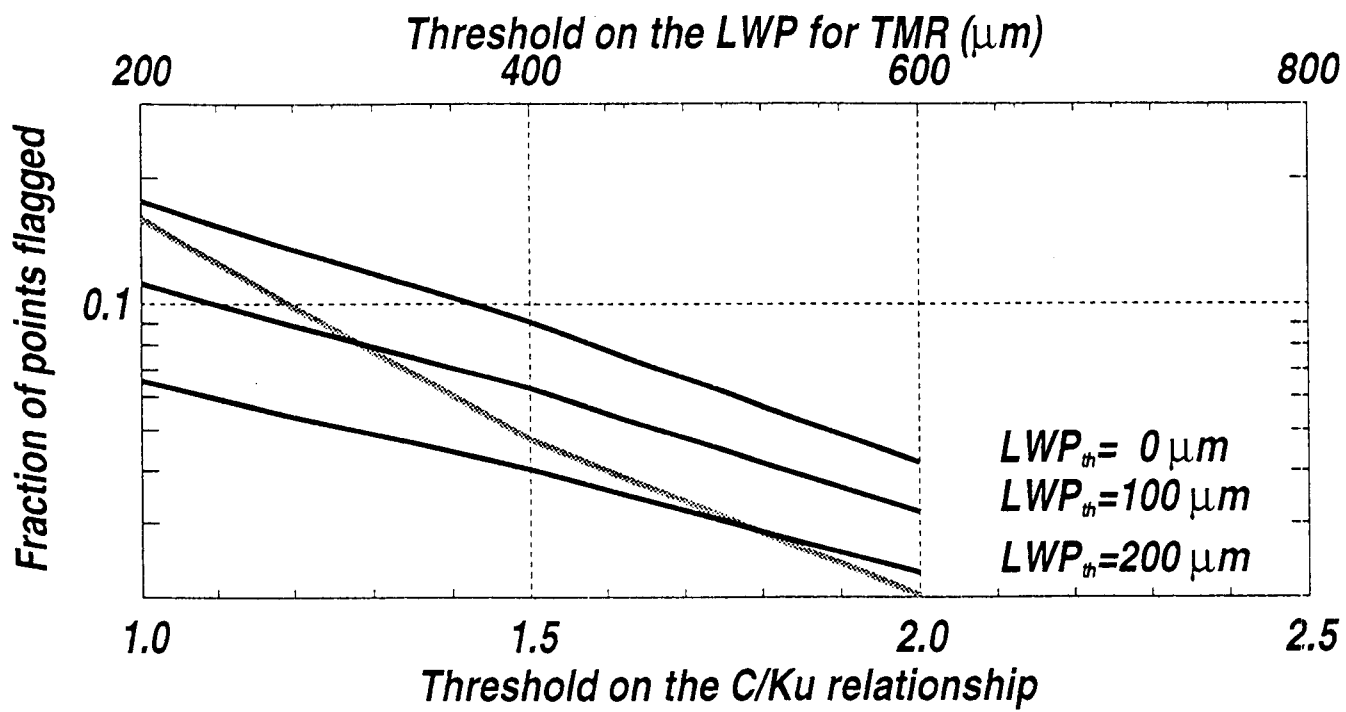


Fig 5

dc & vz 08/06/98